Research Article

Porous Silicates Modified with Zirconium Oxide and Sulfate Ions for Alcohol Dehydration Reactions

Heriberto Esteban Benito,[1] **Ricardo García Alamilla,**[1] **Juan Manuel Hernández Enríquez,**[1]
Francisco Paraguay Delgado,[2] **Daniel Lardizabal Gutiérrez,**[2] **and Pedro García**[3]

[1]*Instituto Tecnológico de Ciudad Madero, Prolongación Bahía de Aldair, Avenida de las Bahías,*
 Parque de la Pequeña y Mediana Industria, Altamira, TAMPS, Mexico
[2]*Centro de Investigación en Materiales Avanzados (CIMAV), Avenida Miguel de Cervantes 120, 31109 Chihuahua, CHIH, Mexico*
[3]*División Académica de Ciencias Agropecuarias, Universidad Juárez Autónoma de Tabasco, Carretera Teapa Km 25,*
 Ranchería la Huasteca, 86600 Centro, TAB, Mexico

Correspondence should be addressed to Ricardo García Alamilla; ricardogarcia.alamilla@yahoo.com.mx

Porous silicates were synthesized by a nonhydrothermal method, using sodium silicate as a source of silica and cetyltrimethylammonium bromide as a template agent. Catalysts were characterized using thermogravimetric analysis, N_2 physisorption, X-ray diffraction, FTIR spectroscopy, pyridine adsorption, potentiometric titration with *n*-butylamine, scanning electronic microscopy, and transmission electronic microscopy. The surface area of the materials synthesized was greater than $800 \, m^2/g$. The introduction of zirconium atoms within the porous silicates increased their acid strength from −42 to 115 mV, while the addition of sulfate ions raised this value to 470 mV. The catalytic activity for the dehydration of alcohols yields conversions of up to 70% for ethanol and 30% for methanol.

1. Introduction

In recent years, there has been an increase in the study of solid acid catalysts for use in industrial catalytic reactions, such as cracking, isomerization, and alkylation of light paraffin, in order to improve the quality of fuels [1–3]. The new generation of solid catalysts can be reused, a money-saving advantage that avoids the environmental contamination associated with commercial catalysts, such as H_2SO_4, HF, $AlCl_3$, BF_3, and H_3PO_4, which the chemical industry has relied upon for a long time now [1, 4]. Of the solid acids studied in recent years, zeolites (HY, Beta, H-Mordenite, and ZSM-5), SiO_2-Al_2O_3 mixed oxides, and metal oxides, such as ZrO_2, TiO_2, SnO_2, and Fe_2O_3, have received the most attention. The magnitude of their acid strength can be increased by modification with SO_4^{-2}, WO_4^{-2}, and MoO_4^{-2} [5–9] ions. These solid acid catalysts have given good results in the fine chemical industry [10]. Current catalyst research has focused on the synthesis of SBA and MCM types of mesoporous silica. These types of materials allow the reactants to diffuse and then transform the reactants on their numerous active centers, thereby yielding increased reaction conversion percentages [11, 12]. Unfortunately, these mesoporous materials have a low thermal stability and poor surface acidity, limiting their application as a catalyst or support. The literature reports that the introduction of transition metals, such as Ti, Zr, V, Fe, Cu, and Mo, within the structure of some mesoporous silicates, plus their impregnation with oxoanions and/or polyacids, increases their acidity and improves the catalytic performance in epoxidation, transesterification, and alcohol dehydration reactions [13–16]. The dehydration of alcohols requires materials with acid sites. Fu et al. [17] studied the decomposition of methanol on H-ZSM-5, H-Y zeolite, γ-Al_2O_3, and $Ti(SO_4)_2/\gamma$-Al_2O_3 supports over a temperature

range of 127 to 327°C. Tang et al. [18] used methanol as a model molecule to evaluate the catalytic activity of a ZSM-5/MCM-41 material at temperatures of 170 to 310°C; they reported high activity, selectivity, and stability for methanol dehydration to DME at 210°C. Trakarnpruk [15] analyzed the catalytic activity of CeHPW/MCM-41 and CuHPW/MCM-41. These materials, used to dehydrate ethanol at 200–350°C, presented selectivity for diethyl ether at 300°C. The selectivity for ethylene increases with the temperature and reduced the selectivity for ether. Ahmed et al. [19] synthesized zirconia materials and impregnated them with different weight percentages of sulfate ions (5–30 wt.%) before evaluating their activity in ethanol dehydration at 380°C. Ethylene selectivity was 100% in all samples.

In the present work, the acid properties of a mesoporous silicate were modified with zirconium oxide using a quick, straightforward synthetic route [20]. Furthermore, two different methods were used to impregnate the resulting materials with a theoretical weight of 12% of sulfate ions before testing them for ethanol and methanol decomposition.

2. Materials and Methods

2.1. Material Synthesis. The mesoporous zirconium silicate materials were synthesized according to techniques reported by Sepehrian et al. [20]. In summary, the synthesis involved dissolving cetyltrimethylammonium bromide (CTMABr, Aldrich, 99%) in distilled water. The mixture was stirred for 15 min before adding a known mass of sodium silicate ($Na_2O_7Si_3$; Aldrich) and stirring strongly for a further 30 min at room temperature. The resulting solution had a pH of 12 which was adjusted to 9 with additions of 2 M H_2SO_4. The white precipitate obtained was filtered, washed, and dried in oven at 80°C for 48 h. The resulting material was calcined at 600°C for 6 h in in an extra-dry air flow. This pure mesoporous silicate was designated SM. A zirconium silicate was then synthesized following the same method as the SM; after adjusting the pH of the alkaline mixture, a zirconium oxychloride solution ($ZrOCl_2·8H_2O$; Merck, 98%) was added dropwise and under constant stirring for 4 h at room temperature.

This yielded a white precipitate which was filtered, washed, and dried under the same conditions as the SM material. A portion of this solid product was impregnated using a solution of 2 M H_2SO_4, which provided a theoretical sulfate ion (SO_4^{-2}) content of 12 wt.%, and the incipient wetness technique; the product was then dried at 80°C for 12 h. Samples with and without sulfate ion impregnation, named 12SZSM and ZSM, respectively, were calcined at 600°C for 6 h in a tubular furnace. To evaluate the effect of calcination temperature on catalytic activity, another portion of the ZSM material was impregnated under the same conditions as 12SZSM but this time it was calcined at 500°C for 3 h; the catalyst obtained was named 12SZSM-2. A diagram of the synthetic route is shown in Scheme 1.

2.2. Materials Characterization. The weight loss of unmodified and modified silicate hydroxides was determined by thermogravimetric analyses (TG and DTG), the crystalline properties of all samples were determined by X-ray diffraction, and samples were studied in two 2θ ranges, low angle from 1 to 10° and high angle from 20 to 80°. The specific surface area of each catalyst was determined according to the Brunauer-Emmett-Teller (BET) adsorption isotherm equations, while average pore diameters and total pore volumes were measured using the BJH method. The nature and acid strength were determined by pyridine adsorption analysis using FTIR and potentiometric titration with *n*-BTA. Finally, the morphology was investigated through electron microscopy techniques (SEM and TEM).

2.3. Catalytic Activity Measurements. The dehydration of ethanol was realized at 300, 325, and 350°C, while methanol decomposition was carried out at 340°C. The catalytic test of the materials was performed in a homemade microactivity system operating at atmospheric pressure and under continuous flow. The reaction system consists of a quartz tubular microreactor in which 100 mg of catalyst was placed. Reaction products were analyzed in a Shimadzu-FID gas chromatogram equipped with a capillary column SPB-1 of 30 m × 0.32 mm and 1 μm FILM supplied by SUPELCO.

3. Results and Discussion

3.1. Thermal Analysis. Figure 1 shows the thermogravimetric analysis from the synthesized precursor materials. The results showed that the mass loss occurred in three stages. In the first stage, the catalytic precursors SM, ZSM, and 12SZSM showed a weight loss of about 5% of their initial mass and in the case of 12SZSM-2 it was 10%. These changes occurred between room temperature and 100°C and are attributed to the removal of physically absorbed water [21]. The second stage of weight loss occurred between 100 and 350°C; this was due to template agent decomposition [22]. The final stage of weight loss occurred between 350 and 650°C. The SM silicate lost only 6% of its total weight over this temperature range, indicating that a greater amount of organic matter was removed at lower temperatures. Whereas ZSM and 12SZSM lost 15 and 19%, respectively, this weight loss is still attributed to the combustion of residual organic matter and also to the dehydroxylation of precursors, promoting the formation of Si-O-Si bonds [21].

In curves from derivative thermogravimetric analysis (DTG), multiple signals emphasizing different weight losses were observed for all materials according to the heat treatment used in synthesis. For SM there were three intense signals centered at 50, 230, and 310°C producing a weight loss of 37%. In the ZSM material, signals from the DTG curve are centered at 56, 279, and 331°C leading to a weight loss of 22% and there were only two broad signals centered at 56 and 319°C for 12SZSM. The observed shift in the maximum of the DTG curves for SM, ZSM, and 12SZSM is attributed to amino groups produced by decomposition of the template agent which then interact strongly with zirconium species and so require higher decomposition temperatures. Similar behavior was recently reported by de Souza et al. [21].

On the other hand, 12SZSM-2 lost 15 wt.% when heated from room temperature to 150°C and an intense signal
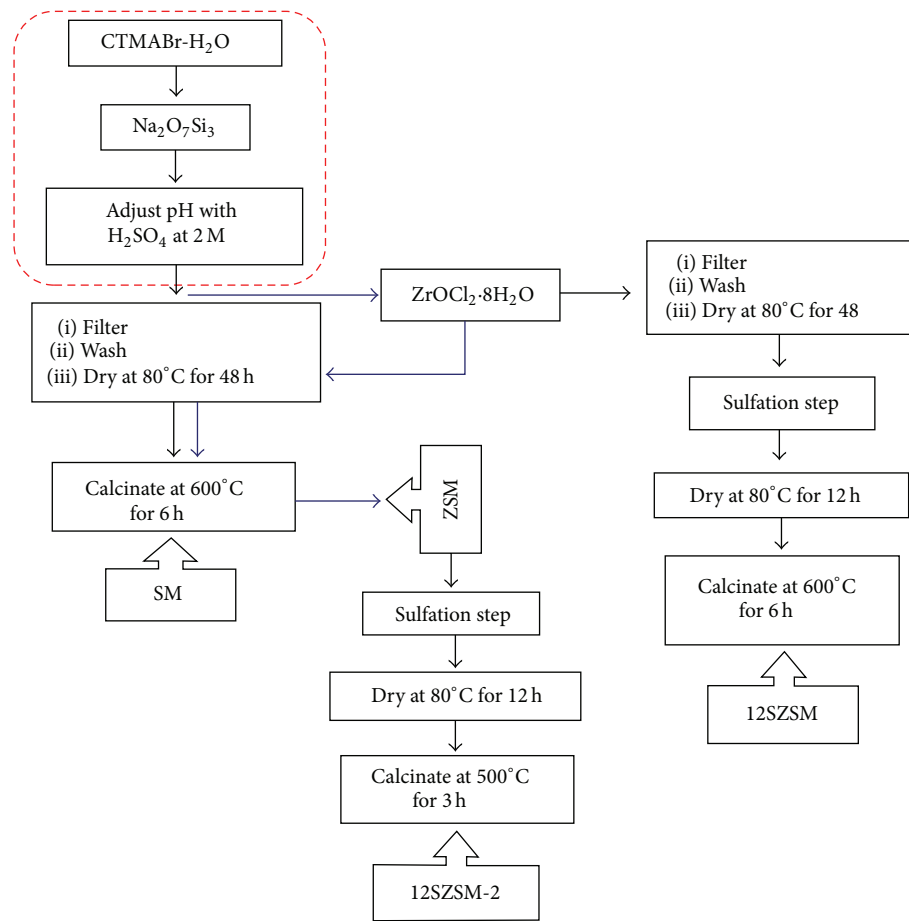
SCHEME 1: Materials synthesis process.

centered at 80°C was observed in the DTG curve. This signal can be attributed to the elimination of water occluded inside the pore structure of the material. The DTG curve for 12SZSM presented a broad signal starting at 450°C associated with the beginning of the evacuation of the sulfate ion; this signal had a maximum value at 572 and 650°C, possibly indicating the existence of different sulfate species. The total weight loss was approximately 40% for all materials except for 12SZSM-2, which presented a loss of only 25%.

3.2. X-Ray Diffraction. The XRD patterns of the materials are shown in Figure 2 for low and high angles. Figure 2(a) shows low-angle XRD patterns which reveal intense diffraction at 2.5° that is characteristic of a hexagonal symmetry arrangement similar to that of MCM-41 in the case of SM [23]. However, the intensity of this signal decreases and shows a slight shift for ZSM, 12SZSM, and 12SZSM-2, which may be due to the formation of zirconia crystals on the silicate surface and a strong interaction caused by sulfate ions. These processes degenerate the silicate's porous arrangement. This kind of damage is most evident in the material 12SZSM-2 which may be due to its higher content of sulfate ions (Figure 1(d)); despite this fact, the material still presents some degree of porosity (Figure 3). Jiang et al. [24] also observed

this phenomenon when they increased the zirconium content in MCM-41.

Figure 2(b) shows the high-angle XRD pattern with three diffraction peaks at around 30, 50, and 60° on the 2θ scale, representing a zirconium oxide with a tetragonal structure [10, 25]. When sulfate ions were added to the ZSM sample, the peaks characteristic of the tetragonal phase of zirconia disappeared; it became an amorphous phase. The high-angle XRD pattern for 12SZSM-2 revealed equivalent behavior as it only presented one peak at around 50° on the scale.

All XRD patterns had a broader intensity around 22° in 2θ, which is characteristic of amorphous silica [26]. This peak decreased in samples impregnated with sulfate ions, while the XRD pattern for pure silicate presented a small diffraction peak at 31°, identified as silica.

3.3. Texture Properties. The nitrogen adsorption-desorption isotherms and porous diameter distributions acquired from materials calcined at 600°C are shown in Figures 3(a) and 3(b), respectively. The determined textural parameters from BET and BJH are shown in Table 1. Figure 3(a) shows isotherms type IV for all materials. This is a typical performance from microporous materials with hysteresis cycle type H3, which is characteristic for the materials with lamellar
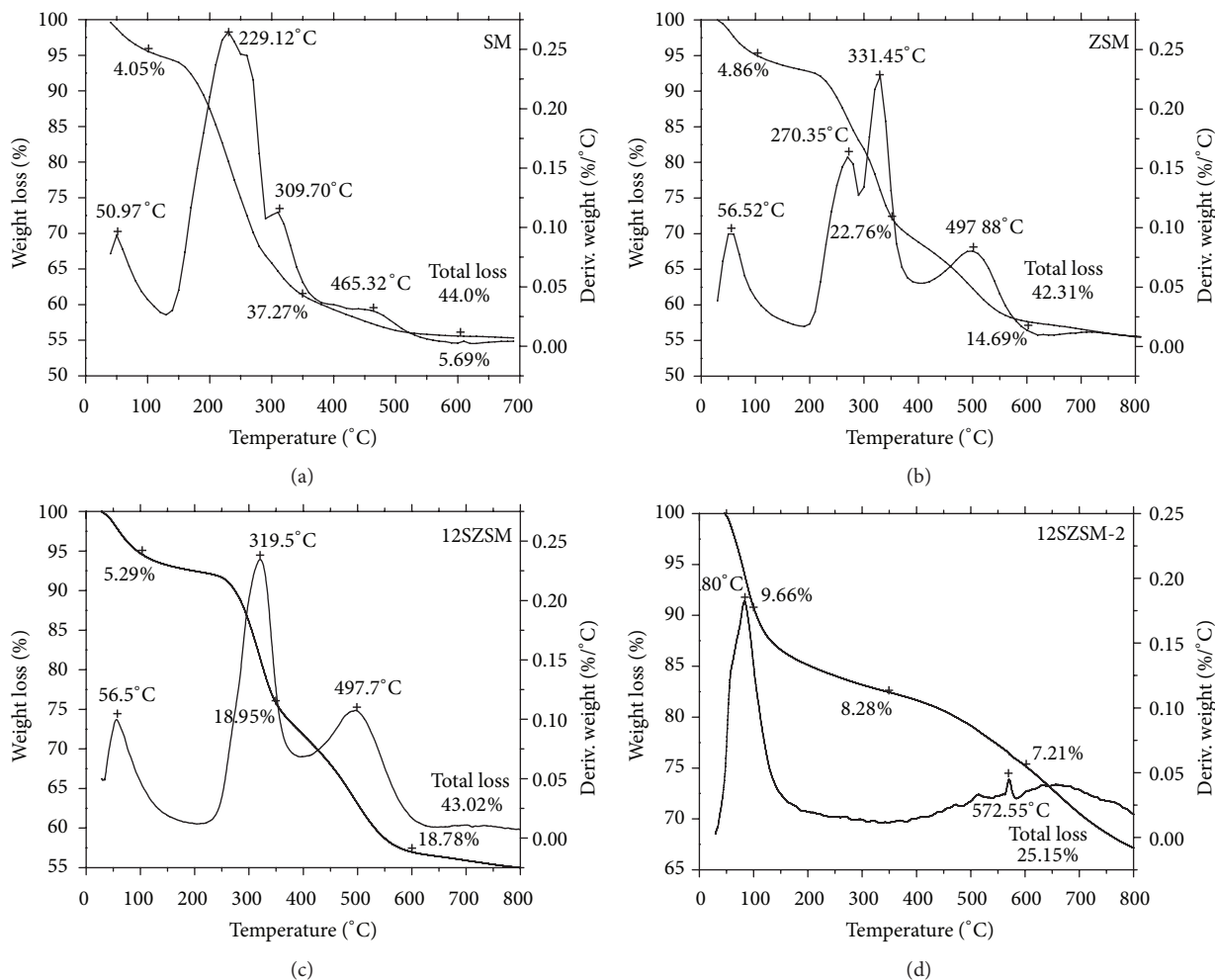
Figure 1: Thermal analysis: TG-DTG of the materials (a) SM, (b) ZSM, (c) 12SZSM, and (d) 12SZSM-2.

Table 1: Textural properties of the catalysts.

Materials	Surface area (m^2/g)	Pore diameter (Å)	Pore volume (cm^3/g)
ZSM	820	20	0.72
12SZM	802	17	0.48
12SZM-2	670	19	0.58

type particles; this has slits type with nonuniform porous size [27]. The addition of zirconium atoms and sulfate ions in the synthesis of porous silicate reduces slightly the specific area; this phenomenon is associated with zirconium oxide formation (see Figure 2(b)). The porous volume and diameters values for the ZM41, 12SZM41, and 12ZM41-2 samples do not show significant change (see Table 1).

3.4. Particle Morphology and Elemental Composition. Figure 4 shows SEM images acquired by secondary electrons of the materials synthesized. All samples presented particle conglomeration, with no definitive geometrical shape and

particle size. The images presented in Figure 4 are from typical porous type particles; thus, undefined edges are observed as in the case of crystalline particles. The sample 12SZSM and 12SZSM-2 show a few particles with approximately 0.3 μm of size and apparently more solid, it could be due to the sequence synthesis of the material. These morphologies confirm the formation of porous silicates with a high specific surface area, in concordance with XRD and BET.

Figure 5 shows the EDS elemental analysis spectra for samples impregnated with Zr and S (12SZSM, 12SZSM-2), respectively. The spectra show the presence of Si, O, Zr, and S elements, and they confirm the incorporation of these elements in the structure of mesoporous silicates. However, the sulfur content in 12SZM is low (Table 2); this could be because the majority of species were eliminated during thermal treatment (600°C). This result agrees with the thermogram weight changes presented in Figure 1.

Figure 6 shows bright-field TEM images for the silicate materials synthesized in this work. All images show a typical porous arrangement similar to MCM-41 material with channels, which are in concordance with XRD at low angle pattern intensity presented in Figure 2(a). The samples SM
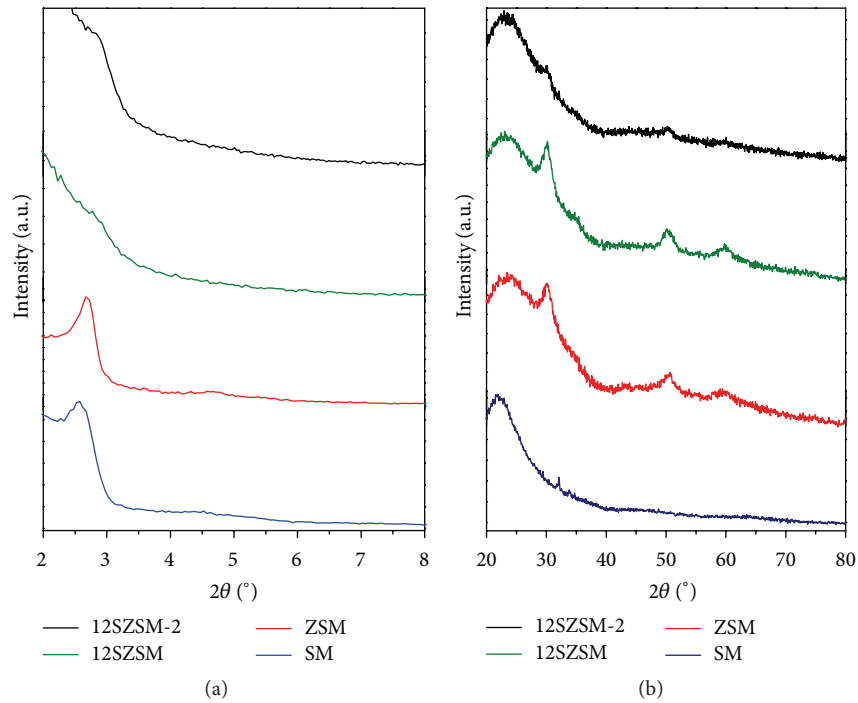
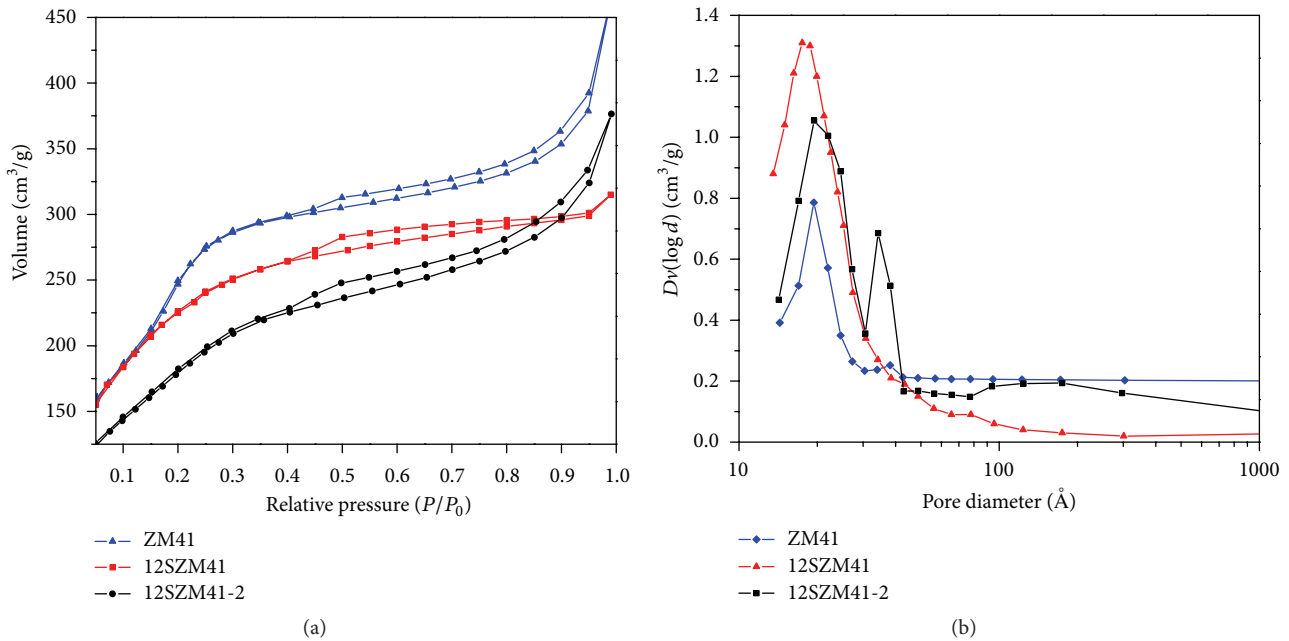FIGURE 2: X-ray diffraction of silica mesoporous materials: (a) low angles and (b) high angles.

FIGURE 3: (a) Adsorption isotherm of mesoporous materials and (b) pore size distribution.

and SZM show uniform layer thickness due to the uniform contrast; elongated straight channel arrangements for both materials can be noticed. In the case of 12SZSM and 12SZSM-2 samples, the images show nonuniform contrast, due to their thickness changes or compound. In the case of 12SZSM and 12SZSM-2 samples, the images shown non-uniform contrast, due to their thickness changes or compound, because these

materials have Zr and S elements according to the synthesis sequence (Scheme 1). The channels in the sample 12SZSM are continuous curved; it could be due to the Zr and/or S incorporated in the porous material wall growing. This type of channel is not noticed in the SM sample, due to the pure silicate compound; its diameter is around 20 Å, but in the case of 12ZSM the diameter is around 15 Å. This image confirms
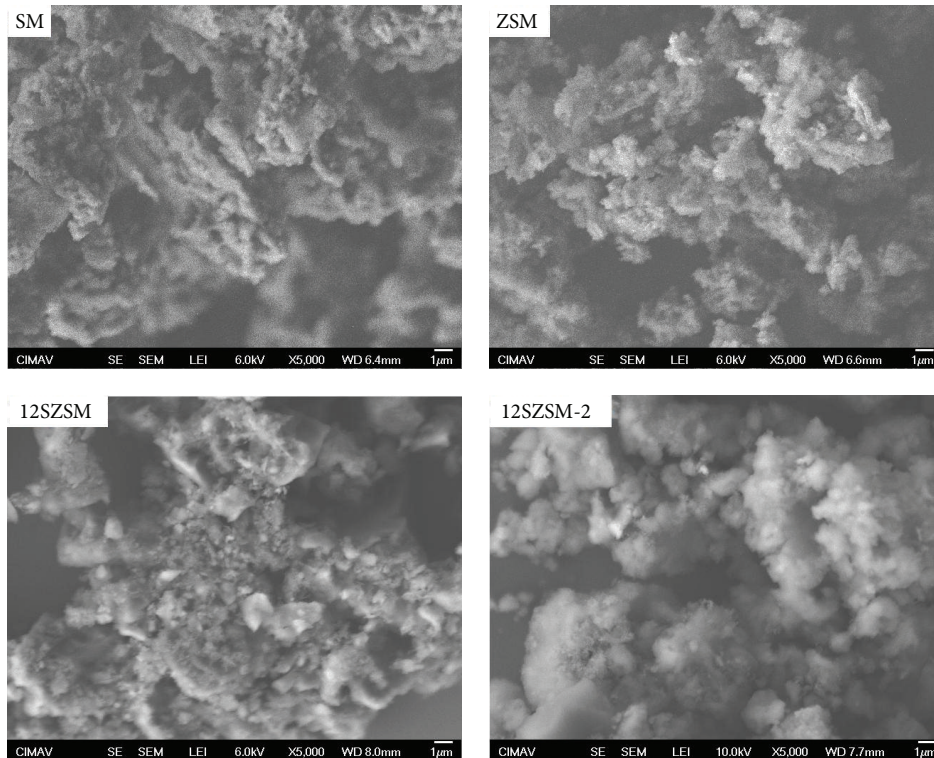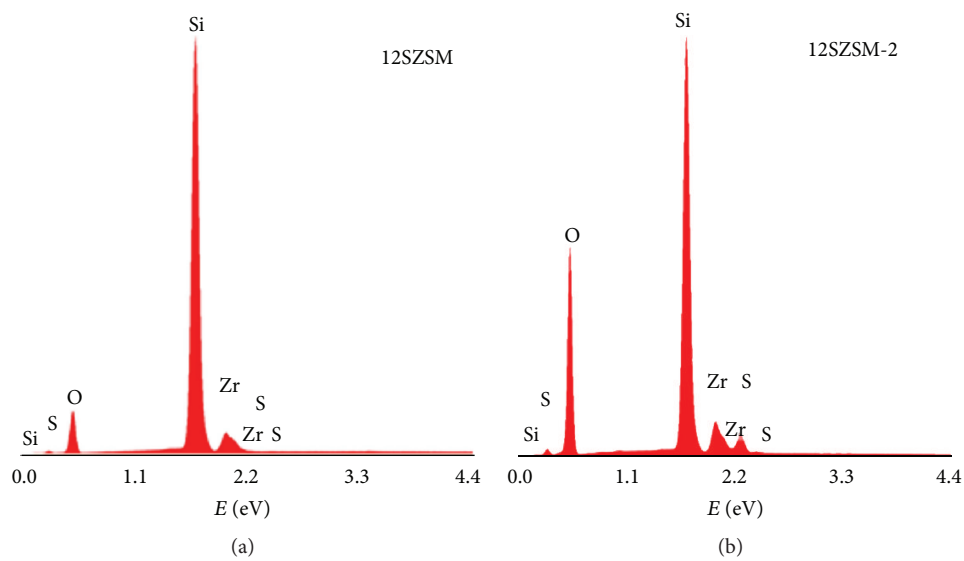
FIGURE 4: SEM micrograph by secondary electrons.

FIGURE 5: Energy Dispersive Spectroscopy (EDS) of sulfated materials.

the shape and does not clearly define XRD pattern intensity in Figure 2(a) for this sample, because the channels are always curved. According to the micrographs, these silicate materials studied are mesoporous.

3.5. Infrared Spectroscopy. FTIR spectra for the study materials are shown in Figure 7. The signal observed at 460 cm^{-1} is attributed to metal-oxygen binding, specifically to Si-O

and Zr-O bonds found in the prepared silicates [28]. The signals at 810 and 1080 cm^{-1} belong to symmetric and asymmetric molecular oscillations produced by Si-O-Si bonds; these peaks were observed for all samples [24]. Said et al. [28] reported that signals for sulfate ions were found at 1053, 1120, and 1224 cm^{-1} in a sulfated zirconium material. However, in the present study these signals may have overlapped with signals from zirconium silicate. To provide support for this
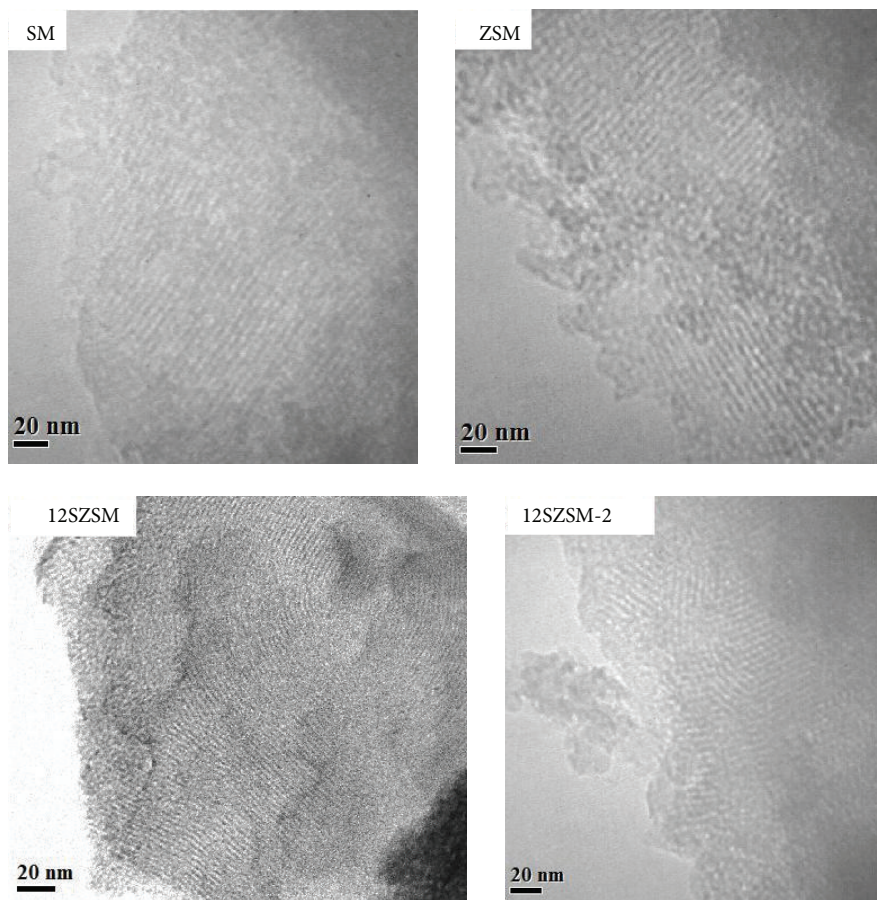
FIGURE 6: Bright field TEM micrograph of silicate mesoporous.

TABLE 2: Elemental composition of sulfated materials.

12SZSM		12SZSM-2	
Element	Atomic %	Element	Atomic %
O K	59.98	O K	63.72
Si K	36.21	Si K	31.04
Zr L	2.92	Zr L	2.98
S K	0.89	S K	2.26

idea, a sodium sulfate (Na_2SO_4) FTIR spectrum was used as a reference to identify sulfate functional groups. This spectrum showed strong signals at 610 and 1089 cm^{-1}, which are associated to S-O bonds [29]. However, the sulfates free zirconium silicate show intense bands and the same wavenumber IR range. This situation causes a great difficulty to identify sulfate groups in 12SZSM and 12SZSM-2 materials, due mainly at low sulfate content. Contrastingly, the peak located at 1080 cm^{-1} for 12SZSM-2 is more intense than that of 12SZSM; consequently this correlates with the greater quantity of sulfate ions retained in the first material. This result was corroborated by EDS analysis (Figure 5). The difference is attributed to the lower temperature of calcination associated to the material 12SZSM-2.

3.6. *n-Butylamine Potentiometric Titration.* Figure 8(a) shows the variation in the maximum acid strength (MAS) developed by the pure silicate and the silicates impregnated with Zr and S. The MAS was determined by potentiometric titration with *n*-butylamine [30]. From the results, pure silicate, SM, showed only very weak acid sites; a value of −42 mV was recorded for the MAS. The materials which incorporated zirconium atoms in their synthesis presented a MAS of 115 mV; this is a change of four orders of magnitude compared to pure silicate. To increase the total acidity and MAS, the ZSM material was impregnated with H_2SO_4. These processes helped to improve the MAS developed by 12SZSM and 12SZSM-2, with values of 153 and 470 mV, respectively. Only a slight difference in maximum acid strength was observed between ZSM and 12SZSM (a 40 mV increase). This is related to the concentration of sulfate ions retained on the material surface after calcination at 600°C process which leads to the removal of SOx species [19] due to the high temperatures used to form the mesoporous silicate (see Figure 1). The sulfation and calcination temperature has a strong influence on the remanent concentration of sulfate ions, this was corroborated by the acid strength developed by 12SZSM-2 and 12SZSM. The former material had the highest MAS, as shown in Figure 8(b), while contrastingly 12SZSM

TABLE 3: Ethanol dehydration over mesoporous catalysts.

Materials	$T = 300°C$			$T = 325°C$			$T = 350°C$		
	X_A (%)	$SC_2^=$ (%)	S_E (%)	X_A (%)	$SC_2^=$ (%)	S_E (%)	X_A (%)	$SC_2^=$ (%)	S_E (%)
SM	0	0	0	0	0	0	1	100	0
ZSM	73	71	29	94	90	9	100	96	4
12SZSM	76	56	43	80	76	24	95	86	14
12SZSM-2	100	99	0.5	—	—	—	—	—	—

X_A = conversion.
$SC_2^=$ = selectivity to ethylene.
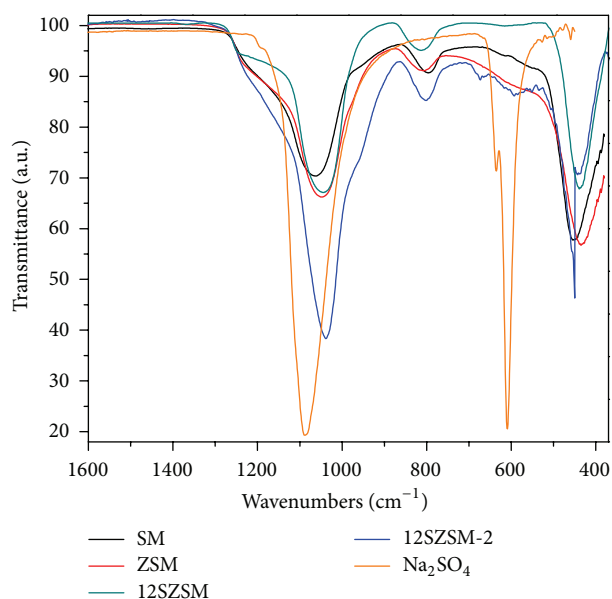S_E = selectivity to diethyl ether.

FIGURE 7: IR spectra of the material prepared and the reference Na_2SO_4.

has strong and weak acid sites, in accordance with the classification reported by Pizzio et al. [30]. These classifications are $E > 100$ mV (strong acid sites), $0 < E < 100$ mV (strong), $-100 < E < 0$ mV (weak), and $E < -100$ mV (very weak).

3.7. FTIR Spectroscopy of Pyridine Adsorption.
A pyridine adsorption experiment for two samples (ZSM and 12SZSM) was performed in order to identify the type of acidity; the results are shown in Figure 9. Both materials exhibited Lewis acid sites at 1445, 1580, 1595, and 1609 cm^{-1}, which are caused by the presence of zirconium atoms in the mesoporous silicate structure [31, 32]. Impregnating pure silicate material with sulfate ions in the precursor phase slightly modified the acid type of the resultant 12SZSM material. This is because sulfate groups in association with water molecules generate Brønsted type acid sites, producing a weak signal at around 1544 cm^{-1} [33], as well as a signal at 1490 cm^{-1} attributed to acid sites. In general, the ZSM material presented Brønsted-Lewis type acid sites from room temperature up to 200°C and 12SZSM retained pyridine at temperatures over 400°C.

3.8. Catalytic Activity

3.8.1. Ethanol Dehydration Reaction. In order to investigate the catalytic behavior of the samples, the ethanol dehydration reaction was carried out. The alcohols decomposition is a model reaction to determine the acid-base nature of catalytic materials and can serve as a characterization technique to evaluate the relative acidity between catalysts. It has been reported in the literature that the ethanol decomposition reaction can follow three possible routes: (1) intramolecular dehydration that produces ethylene, (2) intermolecular dehydration to generate diethyl ether, and (3) alcohol dehydrogenation to produce acetaldehyde [34]. It is known that, under inert atmosphere, the alcohol dehydration reactions take place through acid sites, whereas the dehydrogenation reaction is catalyzed by basic sites [35]. Thus, reaction selectivity is a measure of the relative amounts of each site type in the catalyst. The results are presented in Table 3. Pure mesoporous silicate (SM) did not show any catalytic activity in the range of temperatures studied due to a lack of acid sites, whereas the silicates modified with zirconium and sulfated ions were active (ZSM, 12SZSM, and 12SZSM-2). Catalysts show high conversions > 70%. The activity order at 250°C is the following: 12SZSM-2 > 12SZSM > ZSM. It is clear that the variation in catalytic activity is correlated with the acid sites amount developed on the samples, data that were obtained by potentiometric titration with *n*-butylamine (Figure 8). The nature, density, and strength of surface acid sites of these materials could be related to the presence of zirconium atoms and amount of sulfate ions retained in the mesoporous silicate after calcination process. A predominance of acid sites in the synthesized samples can be observed, since the reaction leads exclusively to the formation of dehydration products, ethylene and diethyl ether, the former being favored in all cases. Clearly this reaction is very sensitive to the change in the operation temperature, where a small temperature increase of only 10°C seriously affects the ethanol conversion. The results indicate that the conversion of ethanol and the selectivity toward ethylene increase quickly with temperature rising, but the selectivity of diethyl ether is contrary. At high temperatures, the main reaction product is ethylene which Varisli et al. [36] suggest could result from the decomposition of diethyl ether. Sheng et al. [37] have also reported that high reaction temperatures favor the production of ethylene while at low reaction temperatures diethyl ether formation is favored,
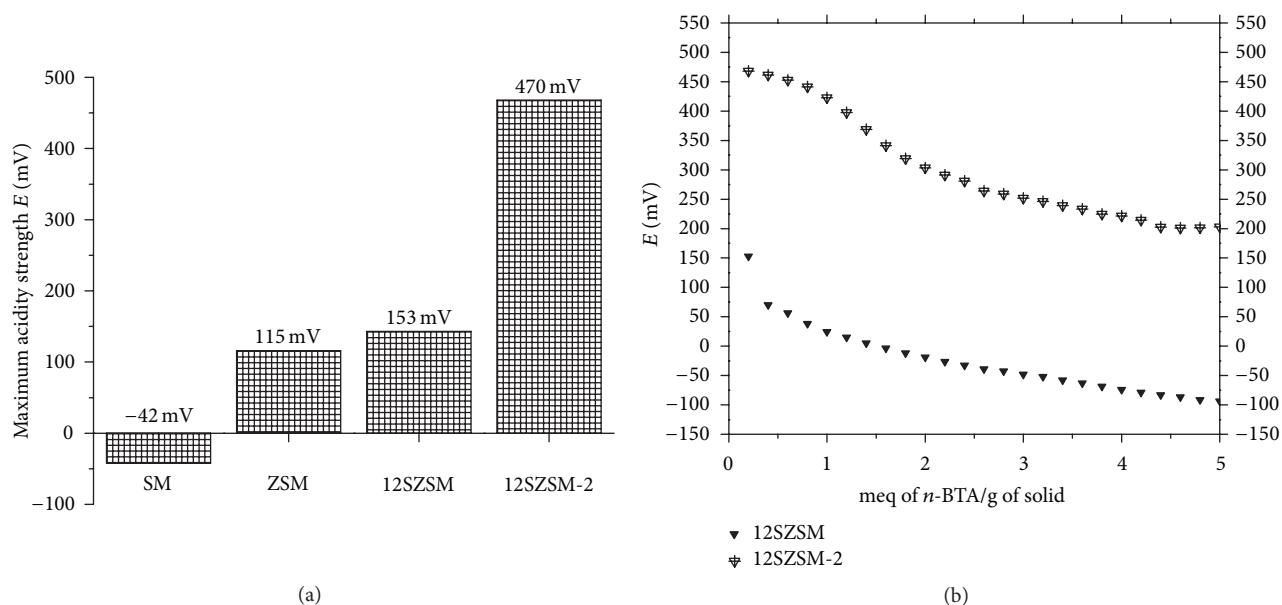
FIGURE 8: Potentiometric titration with *n*-butylamine: (a) maximum acid strength of materials; (b) profile of neutralization of the 12SZSM and 12SZSM-2 materials.
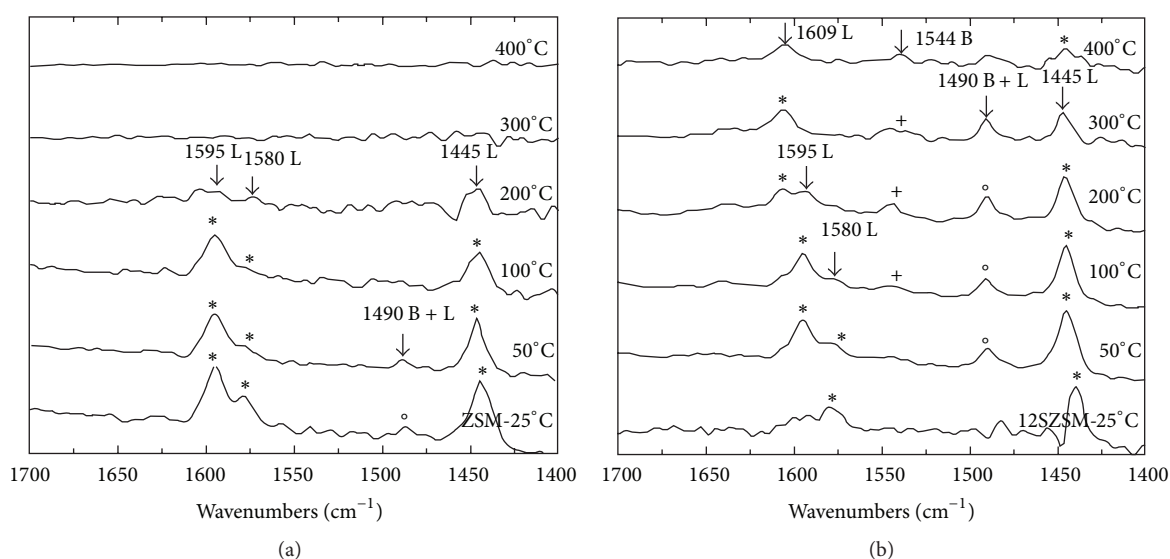

FIGURE 9: FTIR spectrum of pyridine adsorption of ZSM and 12SZSM materials.

consistent with the results obtained in this work. In these tests, there was no acetaldehyde production which indicated that there were no basic sites in the catalysts or if they existed they do not have the sufficient strength to direct the reaction toward the dehydrogenation of the alcohol. All catalysts were stable without any deactivation during 3 h of reaction time.

3.8.2. Methanol Dehydration Reaction. Most studies reported in the literature have focused on the dehydration of alcohols of two or more carbon atoms using solid acid catalysts, concluding that the main reaction product is the corresponding olefin, although in some cases it is indicated that the ether formation can become dominant at low temperatures [38–40]. In the case of methanol, intramolecular dehydration is not possible so the only reaction that can occur is the formation of dimethyl ether and water, although the presence of strong acid sites and high reaction temperatures can lead to obtain lighter products [41]. It is known that the methanol dehydration requires catalysts with strong acidity [17], for this reason the best catalyst of the series (12SZSM-2) was chosen to test its catalytic activity in this reaction. Acidity of this catalyst was enhanced due to the sulfation
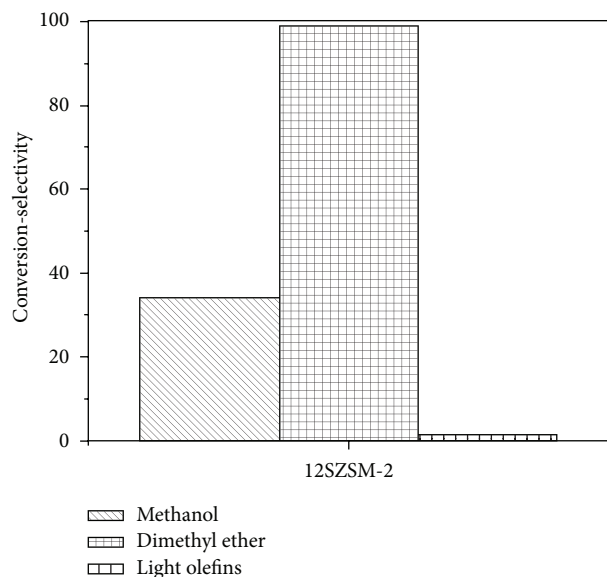
Figure 10: Dehydration of methanol at 340°C.

method which causes more sulfate ions remaining on its surface. The methanol dehydration reaction was evaluated at 340°C because at lower temperatures the catalyst does not show good catalytic performance. Figure 10 shows the catalytic activity of 12SZSM-2 material. The catalyst exhibited moderate activity with conversion around 35% and selectivity toward dimethyl ether formation of 97%. Only trace amounts of light compounds were observed in the products stream (3%). The conversion and selectivity are not changed during 90 min of reaction. This stability can be probably associated with the low reaction temperature and short time of operation. After the reaction, the color of the recovered catalyst was white confirming the absence of coke on its surface.

4. Conclusions

Mesoporous zirconium silicates were prepared by a non-thermal method, modified with sulfur and then thermally treated at 600°C. The resulting products showed a structure similar to that of MCM41, with a surface area of greater than 800 m^2/g, but they collapsed with the introduction of sulfur and promoted the growth of zirconium oxide particles with a tetragonal structure. The acidity and maximum acid strength of the catalytic sites of pure silicate are very poor, but the introduction of zirconium oxide and sulfur increased the strength of the acid sites. Sulfur incorporation augments the number of Brønsted acid sites, which remain firmly anchored to the zirconium silicate, as corroborated by the adsorption and retention of pyridine in the acid sites at temperatures above 400°C. The catalytic activity for ethanol conversion was 70% using materials calcined at 600°C. Whereas methanol dehydration was not possible using the synthesized materials due to the low concentration of acid sites, using 12SZSM-2, methanol dehydration of 30% was achieved while generating dimethyl ether as a single product.

References

[1] P. Gupta and S. Paul, "Solid acids: green alternatives for acid catalysis," *Catalysis Today*, vol. 236, pp. 153–170, 2014.

[2] C.-L. Chen, T. Li, S. Cheng, N. Xu, and C.-Y. Mou, "Catalytic behavior of alumina-promoted sulfated zirconia supported on mesoporous silica in butane isomerization," *Catalysis Letters*, vol. 78, no. 1–4, pp. 223–229, 2002.

[3] C. E. Ramos-Galván, J. M. Domínguez, G. Sandoval-Robles, A. Mantilla, and G. Ferrat, "Isobutane alkylation with C$_4$ olefins on a sulfonic solid acid catalyst system based on laminar clays," *Catalysis Today*, vol. 65, no. 2–4, pp. 391–395, 2001.

[4] C. De Castro, E. Sauvage, M. H. Valkenberg, and W. F. Hölderich, "Immobilised ionic liquids as Lewis acid catalysts for the alkylation of aromatic compounds with dodecene," *Journal of Catalysis*, vol. 196, no. 1, pp. 86–94, 2000.

[5] M. I. Zaki, M. A. Hasan, F. A. Al-Sagheer, and L. Pasupulety, "In situ FTIR spectra of pyridine adsorbed on SiO$_2$-Al$_2$O$_3$, TiO$_2$, ZrO$_2$ and CeO$_2$: general considerations for the identification of acid sites on surfaces of finely divided metal oxides," *Colloids and Surfaces A: Physicochemical and Engineering Aspects*, vol. 190, no. 3, pp. 261–274, 2001.

[6] S. Hayashi and N. Kojima, "Acid properties of H-type mordenite studied by solid-state NMR," *Microporous and Mesoporous Materials*, vol. 141, no. 1–3, pp. 49–55, 2011.

[7] S. Triwahyono, T. Yamada, and H. Hattori, "IR study of acid sites on WO$_3$-ZrO$_2$ and Pt/WO$_3$-ZrO$_2$," *Applied Catalysis A: General*, vol. 242, no. 1, pp. 101–109, 2003.

[8] S. M. Jung and P. Grange, "TiO$_2$–SiO$_2$ mixed oxide modified with H$_2$SO$_4$: II. Acid properties and their SCR reactivity," *Applied Catalysis A: General*, vol. 228, no. 1-2, pp. 65–73, 2002.

[9] S. Damyanova, M. A. Centeno, L. Petrov, and P. Grange, "Fourier transform infrared spectroscopic study of surface acidity by pyridine adsorption on Mo/ZrO$_2$-SiO$_2$(Al$_2$O$_3$) catalysts," *Spectrochimica Acta Part A*, vol. 57, no. 12, pp. 2495–2501, 2001.

[10] V. S. Marakatti, G. V. Shanbhag, and A. B. Halgeri, "Sulfated zirconia; An efficient and reusable acid catalyst for the selective synthesis of 4-phenyl-1,3-dioxane by Prins cyclization of styrene," *Applied Catalysis A: General*, vol. 451, pp. 71–78, 2013.

[11] R. M. Martín-Aranda and J. Čejka, "Recent advances in catalysis over mesoporous molecular sieves," *Topics in Catalysis*, vol. 53, no. 3-4, pp. 141–153, 2010.

[12] M. Mesa, L. Sierra, and J.-L. Guth, "Contribution to the study of the formation mechanism of mesoporous SBA-15 and SBA-16 type silica particles in aqueous acid solutions," *Microporous and Mesoporous Materials*, vol. 112, no. 1–3, pp. 338–350, 2008.

[13] R. V. Sharma, C. Baroi, and A. K. Dalai, "Production of biodiesel from unrefined canola oil using mesoporous sulfated Ti-SBA-15 catalyst," *Catalysis Today*, vol. 237, pp. 3–12, 2014.

[14] Y. Wang, Y. Guo, G. Wang, Y. Liu, and F. Wang, "Synthesis, characterization and catalytic activities of bimetallic modified MCM-41 for epoxidation of styrene," *Journal of Sol-Gel Science and Technology*, vol. 57, no. 2, pp. 185–192, 2011.

[15] W. Trakarnpruk, "Dehydration of ethanol over copper and cerium phosphotungstates supported on MCM-41," *Mendeleev Communications*, vol. 23, no. 3, pp. 168–170, 2013.

[16] I. Jiménez-Morales, J. Santamaría-González, P. Maireles-Torres, and A. Jiménez-López, "Zirconium doped MCM-41 supported WO_3 solid acid catalysts for the esterification of oleic acid with methanol," *Applied Catalysis A: General*, vol. 379, no. 1-2, pp. 61–68, 2010.

[17] Y. Fu, T. Hong, J. Chen, A. Auroux, and J. Shen, "Surface acidity and the dehydration of methanol to dimethyl ether," *Thermochimica Acta*, vol. 434, no. 1-2, pp. 22–26, 2005.

[18] Q. Tang, H. Xu, Y. Zheng, J. Wang, H. Li, and J. Zhang, "Catalytic dehydration of methanol to dimethyl ether over micro–mesoporous ZSM-5/MCM-41 composite molecular sieves," *Applied Catalysis A: General*, vol. 413, pp. 36–42, 2012.

[19] A. I. Ahmed, S. A. El-Hakam, S. E. Samra, A. A. EL-Khouly, and A. S. Khder, "Structural characterization of sulfated zirconia and their catalytic activity in dehydration of ethanol," *Colloids and Surfaces A: Physicochemical and Engineering Aspects*, vol. 317, no. 1–3, pp. 62–70, 2008.

[20] H. Sepehrian, A. R. Khanchi, M. K. Rofouei, and S. W. Husain, "Non-thermal synthesis of mesoporous zirconium silicate and its characterization," *Journal of the Iranian Chemical Society*, vol. 3, no. 3, pp. 253–257, 2006.

[21] L. K. C. de Souza, J. J. R. Pardauil, J. R. Zamian, G. N. da Rocha Filho, and C. E. F. da Costa, "Influence of the incorporated metal on template removal from MCM-41 type mesoporous materials," *Journal of Thermal Analysis and Calorimetry*, vol. 106, no. 2, pp. 355–361, 2011.

[22] M. L. Occelli, S. Biz, and A. Auroux, "Effects of isomorphous substitution of Si with Ti and Zr in mesoporous silicates with the MCM-41 structure," *Applied Catalysis A: General*, vol. 183, no. 2, pp. 231–239, 1999.

[23] A. K. Basumatary, R. V. Kumar, A. K. Ghoshal, and G. Pugazhenthi, "Synthesis and characterization of MCM-41-ceramic composite membrane for the separation of chromic acid from aqueous solution," *Journal of Membrane Science*, vol. 475, pp. 521–532, 2015.

[24] T. S. Jiang, Y. H. Li, X. P. Zhou, Q. Zhao, and H. B. Yin, "Thermal and hydrothermal stability of ZrMCM-41 mesoporous molecular sieves obtained by microwave irradiation," *Journal of Chemical Sciences*, vol. 122, no. 3, pp. 371–379, 2010.

[25] M. Ejtemaei, A. Tavakoli, N. Charchi, B. Bayati, A. A. Babaluo, and Y. Bayat, "Synthesis of sulfated zirconia nanopowders via polyacrylamide gel method," *Advanced Powder Technology*, vol. 25, no. 3, pp. 840–846, 2014.

[26] F. Ghorbani, H. Younesi, Z. Mehraban, M. S. Çelik, A. A. Ghoreyshi, and M. Anbia, "Preparation and characterization of highly pure silica from sedge as agricultural waste and its utilization in the synthesis of mesoporous silica MCM-41," *Journal of the Taiwan Institute of Chemical Engineers*, vol. 44, no. 5, pp. 821–828, 2013.

[27] G. Leofanti, M. Padovan, G. Tozzola, and B. Venturelli, "Surface area and pore texture of catalysts," *Catalysis Today*, vol. 41, no. 1–3, pp. 207–219, 1998.

[28] A. E.-A. A. Said, M. M. Abd El-Wahab, and M. A. El-Aal, "The catalytic performance of sulfated zirconia in the dehydration of methanol to dimethyl ether," *Journal of Molecular Catalysis A: Chemical*, vol. 394, pp. 40–47, 2014.

[29] Q. Guo and T. Wang, "Preparation and Characterization of Sodium Sulfate/Silica Composite as a shape-stabilized phase change material by sol-gel method," *Chinese Journal of Chemical Engineering*, vol. 22, no. 3, pp. 360–364, 2014.

[30] L. R. Pizzio, P. G. Vázquez, C. V. Cáceres, and M. N. Blanco, "Supported Keggin type heteropolycompounds for ecofriendly reactions," *Applied Catalysis A: General*, vol. 256, no. 1-2, pp. 125–139, 2003.

[31] D. Fuentes-Perujo, J. Santamaría-González, J. Mérida-Robles et al., "Evaluation of the acid properties of porous zirconium-doped and undoped silica materials," *Journal of Solid State Chemistry*, vol. 179, no. 7, pp. 2182–2189, 2006.

[32] J. A. Wang, L. F. Chen, L. E. Noreña et al., "Mesoporous structure, surface acidity and catalytic properties of Pt/Zr-MCM-41 catalysts promoted with 12-tungstophosphoric acid," *Microporous and Mesoporous Materials*, vol. 112, no. 1–3, pp. 61–76, 2008.

[33] C. Khatri, M. K. Mishra, and A. Rani, "Synthesis and characterization of fly ash supported sulfated zirconia catalyst for benzylation reactions," *Fuel Processing Technology*, vol. 91, no. 10, pp. 1288–1295, 2010.

[34] X. Zhang, R. Wang, X. Yang, and F. Zhang, "Comparison of four catalysts in the catalytic dehydration of ethanol to ethylene," *Microporous and Mesoporous Materials*, vol. 116, no. 1–3, pp. 210–215, 2008.

[35] A. Haryanto, S. Fernando, N. Murali, and S. Adhikari, "Current status of hydrogen production techniques by steam reforming of ethanol: a review," *Energy and Fuels*, vol. 19, no. 5, pp. 2098–2106, 2005.

[36] D. Varisli, T. Dogu, and G. Dogu, "Silicotungstic acid impregnated MCM-41-like mesoporous solid acid catalysts for dehydration of ethanol," *Industrial & Engineering Chemistry Research*, vol. 47, no. 12, pp. 4071–4076, 2008.

[37] Q. Sheng, S. Guo, K. Ling, and L. Zhao, "Catalytic dehydration of ethanol to ethylene over alkali-treated HZSM-5 zeolites," *Journal of the Brazilian Chemical Society*, vol. 25, no. 8, pp. 1365–1371, 2014.

[38] H. V. Fajardo, E. Longo, E. R. Leite, R. Libanori, L. F. D. Probst, and N. L. V. Carreño, "Synthesis, characterization and catalytic properties of nanocrystaline Y_2O_3-coated TiO_2 in the ethanol dehydration reaction," *Materials Research*, vol. 15, no. 2, pp. 285–290, 2012.

[39] D. Fan, D.-J. Dai, and H.-S. Wu, "Ethylene formation by catalytic dehydration of ethanol with industrial considerations," *Materials*, vol. 6, no. 1, pp. 101–115, 2013.

[40] R. S. Rodrigo, J. M. H. Enríquez, A. C. Mares et al., "Effect of CeO_2 on the textural and acid properties of ZrO_2-SO_4^{2-}," *Catalysis Today*, vol. 107-108, pp. 838–843, 2005.

[41] F. Camacho, S. Delgado, D. Trujillo, J. Del Castillo, and R. Arvelo, "Deshidratación catalítica de metanol en fase vapor," *Ingeniería Química*, vol. 1, no. 148, pp. 113–119, 1980.